iScience

CellPress
OPEN ACCESS

Article

R274X-mutated Phf6 increased the self-renewal and skewed T cell differentiation of hematopoietic stem cells

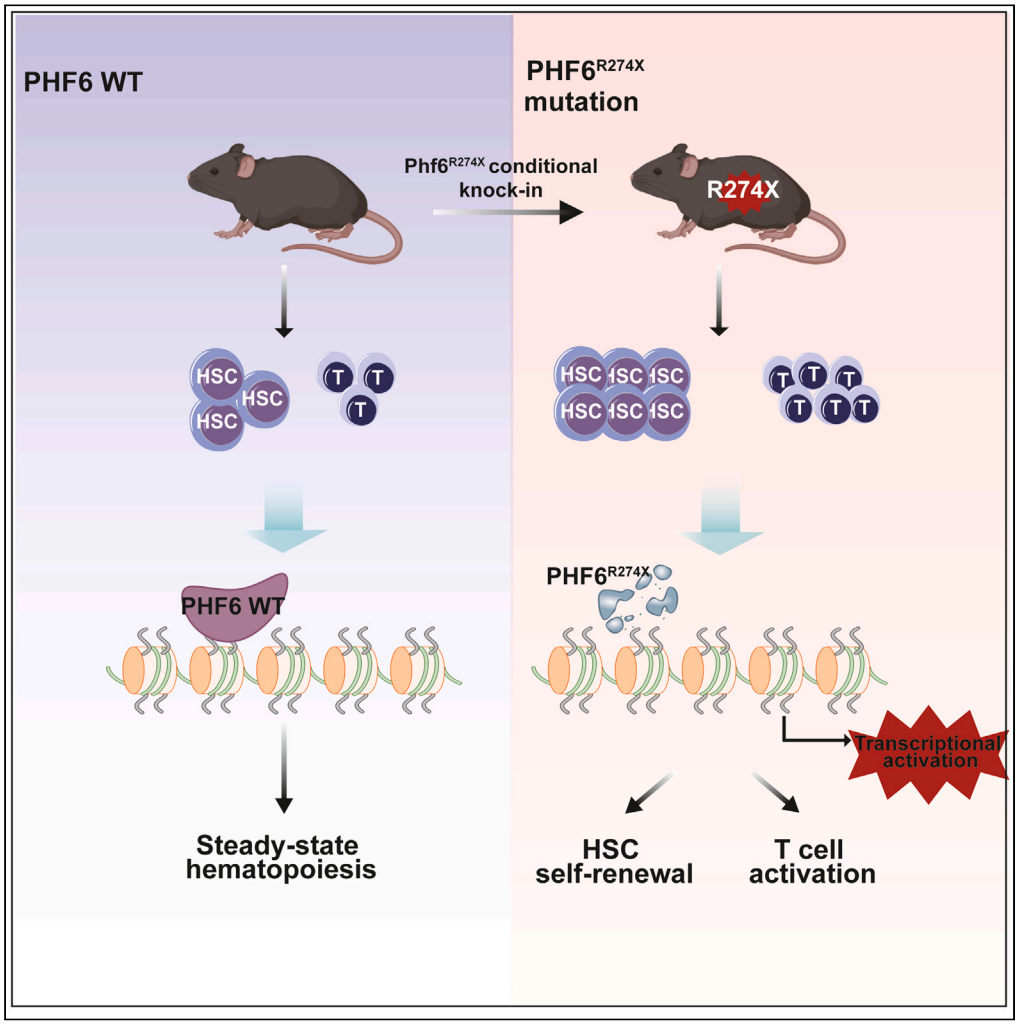

Yanjie Lan, Shengnan Yuan, Tengxiao Guo, ..., Erlie Jiang, Weiping Yuan, Xiaomin Wang

wpyuan@ihcams.ac.cn (W.Y.)
wangxiaomin@ihcams.ac.cn (X.W.)

Highlights

We engineered a conditional *Phf6*^{R274X} knock-in mouse line in hematopoietic system

Phf6^{R274X} mutation expanded HSC/HPC pool *in vivo*

Phf6^{R274X} mutation activated the proliferation and function of T cells *in vivo*

Lan et al., iScience 26, 106817
June 16, 2023
https://doi.org/10.1016/j.isci.2023.106817

iScience

CellPress
OPEN ACCESS

Article

R274X-mutated Phf6 increased the self-renewal and skewed T cell differentiation of hematopoietic stem cells

Yanjie Lan,[1,2,3,6] Shengnan Yuan,[1,4,6] Tengxiao Guo,[1,2,6] Shuaibing Hou,[1] Fei Zhao,[1,2] Wanzhu Yang,[1,2] Yigeng Cao,[1,2] Yajing Chu,[1,2] Erlie Jiang,[1,2] Weiping Yuan,[1,2,*] and Xiaomin Wang[1,3,5,7,*]

SUMMARY

The PHD finger protein 6 (PHF6) mutations frequently occurred in hematopoietic malignancies. Although the R274X mutation in PHF6 (*PHF6*^{R274X}) is one of the most common mutations identified in T cell acute lymphoblastic leukemia (T-ALL) and acute myeloid leukemia (AML) patients, the specific role of *PHF6*^{R274X} in hematopoiesis remains unexplored. Here, we engineered a knock-in mouse line with conditional expression of Phf6^{R274X}-mutated protein in the hematopoietic system (*Phf6*^{R274X} mouse). The *Phf6*^{R274X} mice displayed an enlargement of hematopoietic stem cells (HSCs) compartment and increased proportion of T cells in bone marrow. More *Phf6*^{R274X} T cells were in activated status than control. Moreover, *Phf6*^{R274X} mutation led to enhanced self-renewal and biased T cells differentiation of HSCs as assessed by competitive transplantation assays. RNA-sequencing analysis confirmed that *Phf6*^{R274X} mutation altered the expression of key genes involved in HSC self-renewal and T cell activation. Our study demonstrated that *Phf6*^{R274X} plays a critical role in fine-tuning T cells and HSC homeostasis.

INTRODUCTION

The PHD finger protein 6 (PHF6), a member of PHD family, is an X-linked gene encodes a 365-amino acid protein and is highly conserved in vertebrate species.[1] Structurally, PHF6 possesses two extended atypical PHD-like zinc fingers (ePHD) with a proposed role in gene transcription regulation.[2,3] Intriguingly, unlike other PHD domain-containing proteins, PHF6-ePHD is not able to interact with histones. It's found that PHF6-ePHD2 could bind dsDNA.[2] Nevertheless, it is possible that the ePHD2 domain could interact with RNA, given the role of PHF6 in regulating rRNA synthesis.[4] Moreover, structural analysis of PHF6-ePHD2 showed that mutations in ePHD2 could change the folding of the ePHD2 domain and affect the function of PHF6, possible leading to pathological consequences as suggested in Borjeson-Forssman-Lehmann syndrome (BFLS), T cell acute lymphoblastic leukemia (T-ALL), and Acute myeloid leukemia (AML).[2]

PHF6 was expressed in almost all tissues. Notably, it was high expressed in CD34^{+} precursor cells and B cells.[5] Several mouse models with Phf6 conditional knockout in hematopoietic system showed that loss of Phf6 enhanced hematopoietic stem cell (HSC) self-renewal capacity.[6–8] Interestingly, Phf6 deficiency alone in hematopoietic system was insufficient for leukemia initiation without additional driver gene mutations.[8–10] Somatic mutations of PHF6 have been observed in a variety of hematopoietic malignancies. Studies revealed that the inhibition of PHF6 expression suppressed the growth of B cell acute lymphoblastic leukemia (B-ALL) cells, while enhanced the tumor progression of T-ALL.[11] These findings indicated that PHF6 may have oncogenic and tumor-suppressive functions in a context-dependent manner. The mutation type of PHF6 in hematopoietic malignancies includes deletion, frameshift, nonsense, and missense mutations, and interestingly, with more mutations concentrated in the ePHD2 domain.[12–14] The point mutation c.820C > T (p.R274X), which lead to the truncation of the last 92 amino acids of PHF6, located on ePHD2 domain and frequently occurred in leukemia patients.[14,15] However, the role of *PHF6*^{R274X} in hematopoiesis remain unknown.

In this study, we generated a Vav1 promoter-driven *Phf6*^{R274X} knock-in mouse model (*Phf6*^{R274X} mouse) to elucidate the function of *Phf6*^{R274X} in hematopoiesis *in vivo*. We found that *Phf6*^{R274X} affected self-renewal ability of HSCs and T cells proliferation and activation. Our findings provided a study model for human

[1]State Key Laboratory of Experimental Hematology, National Clinical Research Center for Blood Diseases, Haihe Laboratory of Cell Ecosystem, Institute of Hematology & Blood Diseases Hospital, Chinese Academy of Medical Sciences & Peking Union Medical College, Tianjin 300020, China

[2]Tianjin Institutes of Health Science, Tianjin 301600, China

[3]Department of Neuro-oncology, Cancer Center, Beijing Tiantan Hospital, Capital Medical University, Beijing 100071, China

[4]School of Medical Technology, Xuzhou Medical University, Xuzhou 221004, China

[5]Key Laboratory of Carcinogenesis and Translational Research (Ministry of Education), Department of Lymphoma, Peking University Cancer Hospital & Institute, Beijing 100142, China

[6]These authors contributed equally

[7]Lead contact

*Correspondence: wpyuan@ihcams.ac.cn (W.Y.), wangxiaomin@ihcams.ac.cn (X.W.)

https://doi.org/10.1016/j.isci.2023.106817

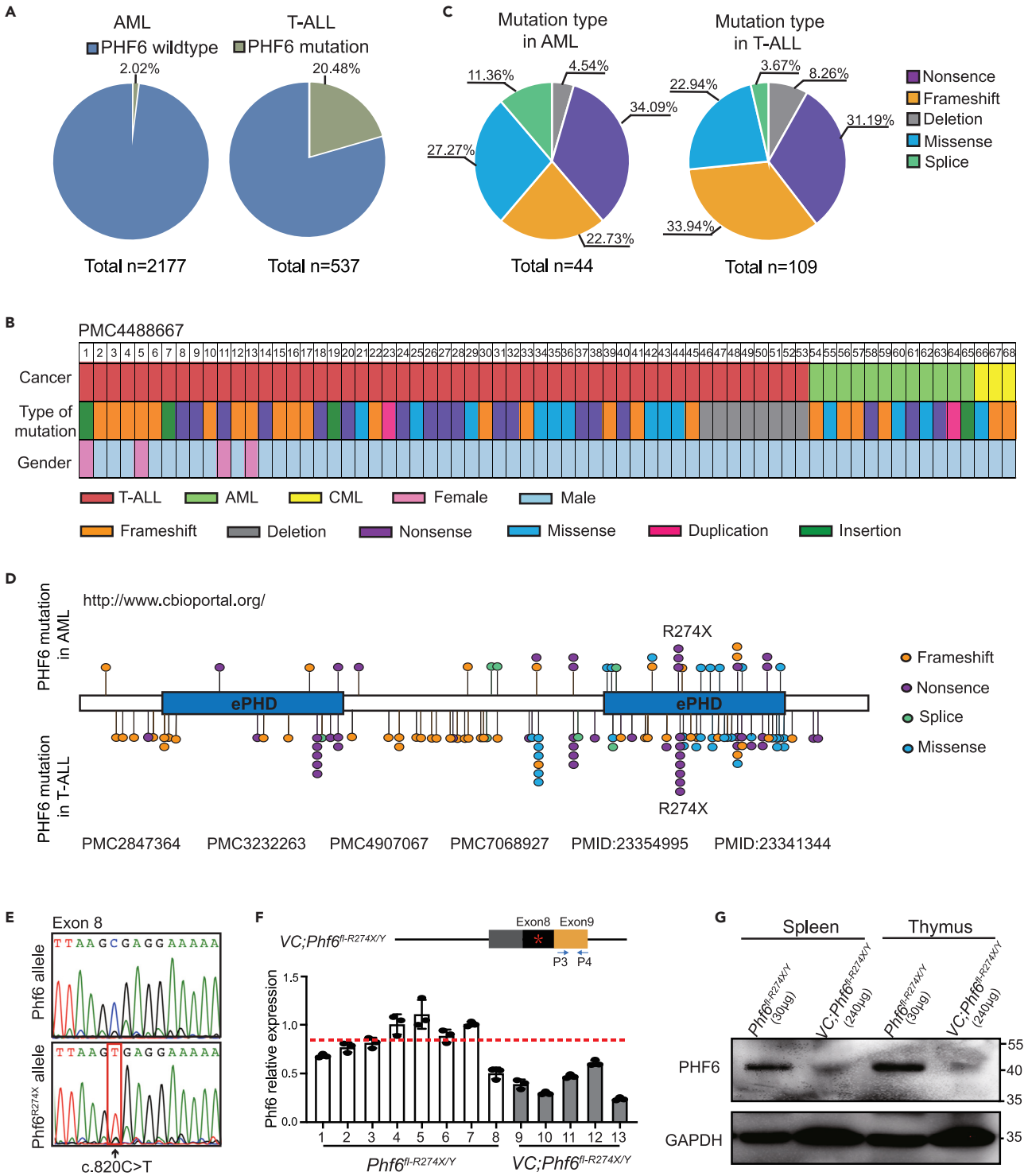

Figure 1. *PHF6*^{R274X} is one of the most common mutations in AML and T-ALL patients

(A) Differential distribution of PHF6 mutations in AML and T-ALL samples. Left panel, the frequency of PHF6 mutations (green) in AML patients. Right panel, the frequency of PHF6 mutations (green) in T-ALL patients.

(B) The mutation types of PHF6 found in 68 leukemia patients in PMC4488667 from Todd, M. A. et al.[20] Each type of mutation is indicated by a unique color.

(C) Nonsense, frameshift, missense, deletion, and splicing variations of PHF6 in AML and T-ALL patients. Left panel, mutation type of PHF6 in AML patients. Right panel, mutation type of PHF6 in T-ALL patients.

Figure 1. *Continued*

(D) Schematic representation of the functional domains and locations of mutations in the human PHF6 protein. Two atypical plant homeodomain (PHD) zinc-finger domains are shown in blue. Each mutation site is indicated by a filled circle with unique color. Mutations in AML samples are shown above the bar, while mutations in T-ALL samples are shown under the bar.

(E) Sequencing analysis of cDNA isolated from BM cells from *Phf6*$^{fl\text{-}R274X/Y}$ and *Vav1-Cre;Phf6*$^{fl\text{-}R274X/Y}$ mice.

(F) RT-PCR showing the mRNA expression of wild-type Phf6 or mutant *Phf6*^{R274X} using primer set P3 and P4 after *Phf6*^{R274X} mutation.

(G) Western blotting analysis of Phf6^{R274X} expression or wild-type PHF6 expression in spleen and thymus cells from *Phf6*$^{fl\text{-}R274X/Y}$ and *Vav1-Cre;Phf6*$^{fl\text{-}R274X/Y}$ mice. Glyceraldehyde-3-phosphate dehydrogenase (GAPDH) was used as a loading control. Data information: in (F) data are shown as the mean ± SD. *p < 0.05, **p < 0.01, and ***p < 0.001 by the Student's *t* test.

blood diseases with *PHF6*^{R274X} and gave a novel insight into the role of *PHF6*^{R274X} mutation in hematopoietic homeostasis.

RESULTS

PHF6^{R274X} mutation frequently occurred in AML and T-ALL patients

To investigate the role of PHF6 in leukemia patients, we analyzed PHF6 mutations in the genetic data of 2177 AML (http://www.cbioportal.org) and 537 T-ALL cases[12,16–19] from different clinical centers. Consistent with previous studies,[12,13] PHF6 mutations occurred in 2.02% (44/2177) of AML patients and 20.48% (110/537) of T-ALL patients (Figure 1A). Notably, we found that most PHF6 alterations presented in T-ALLs, AMLs, and chronic myeloid leukemias (CMLs) were nonsense, frameshift, and deletion mutations (Figure 1B), which accounted for more than half of all PHF6 mutations identified in T-ALL and AML samples (Figure 1C). In addition, we further analyzed details of PHF6 mutations in 44 AML and 109 T-ALL samples. We found that the R274X occurred in 9.68% (3/31) of AML patients with PHF6 mutations and in 7.09% (7/99) of T-ALL patients with PHF6 mutations, indicating that *PHF6*^{R274X} mutation was most frequent in T-ALL and AML patients (Figure 1D).

To investigate the biological role of *PHF6*^{R274X} mutation in hematopoiesis, we engineered a knock-in mouse line with conditional expression of this mutation in the endogenous Phf6 locus (*Phf6*$^{fl\text{-}R274X/fl\text{-}R274X}$ or *Phf6*$^{fl\text{-}R274X/Y}$). To induce the expression of *Phf6*^{R274X} in hematopoietic system, we crossed *Phf6*$^{fl\text{-}R274X/Y}$ knock-in mice with the *Vav1-Cre* transgenic mice, which expressed Cre specifically in blood cells (Figure S1A and S1B). The genotype and sequencing analysis confirmed the engineered C to T transition at exon 8 (c.820C > T) of the Phf6 gene (Figure S1C and 1E) in bone marrow (BM) cells of *Vav1-Cre;Phf6*$^{fl\text{-}R274X/Y}$ mice (*Phf6*^{R274X} mice). Interestingly, although the *Phf6*^{R274X} mRNA expression in BM cells of *Vav1-Cre;Phf6*$^{fl\text{-}R274X/Y}$ mice was approximately 40%–60% of Phf6 in *Phf6*$^{fl\text{-}R274X/Y}$ mice (Figure 1F), the expression of Phf6^{R274X} protein was greatly reduced in spleen and thymus cells of *Vav1-Cre;Phf6*$^{fl\text{-}R274X/Y}$ mice (Figure 1G). We further sorted Lin$^-$ cells from the bone marrow (BM) of *Phf6*$^{fl\text{-}R274X/Y}$ and *Vav1-Cre;Phf6*$^{fl\text{-}R274X/Y}$ mice, and found that the protein of PHF6^{R274X} was greatly reduced in Lin$^-$ cells (Figure S1D). These data indicated that the *Phf6*^{R274X}-mutation containing gene could successfully transcript to mRNA, while the protein translation of Phf6^{R274X} was compromised in hematopoietic cells.

Phf6^{R274X} mutation increases hematopoietic stem/progenitor cells (HSC/HPC) pool in *Vav1-Cre;Phf6*$^{fl\text{-}R274X/Y}$ mice

To investigate the impact of *Phf6*^{R274X} mutation in hematopoiesis, we compared hematopoietic parameters of *Vav1-Cre;Phf6*$^{fl\text{-}R274X/Y}$ mice with their littermate controls. The histologic sections showed no dysplasia in *Vav1-Cre;Phf6*$^{fl\text{-}R274X/Y}$ mice (Figure 2A). The weight of thymus and spleen was similar in *Vav1-Cre;Phf6*$^{fl\text{-}R274X/Y}$ mice and *Phf6*$^{fl\text{-}R274X/Y}$ mice, respectively (Figure S2A-B). No obvious abnormality was observed in peripheral blood (PB) and BM cells from *Phf6*$^{fl\text{-}R274X/Y}$ and *Vav1-Cre;Phf6*$^{fl\text{-}R274X/Y}$ mice stained with Wright-Giemsa staining (Figure 2B). While *Vav1-Cre;Phf6*$^{fl\text{-}R274X/Y}$ mice had slightly higher red blood cell (RBC) counts in PB (Figure 2C). Flow cytometric analysis showed that the proportion of T, B, and myeloid cells in PB was equivalent in *Phf6*$^{fl\text{-}R274X/Y}$ and *Vav1-Cre;Phf6*$^{fl\text{-}R274X/Y}$ mice (Figure 2D). The percentage of T cells was slightly increased in spleen of *Phf6*^{R274X} mice (Figure S2C), while the percentage of T cells in thymus was similar between the two groups (Figure S2D). Notably, the absolute number of T cells in BM was increased (Figure 2E). Carboxyfluorescein succinimidyl ester (CSFE) analysis revealed that *Phf6*^{R274X} increased proliferation of CD4$^+$ and CD8$^+$ T cells (Figure 2F). CD69 and CD25 were T cell activation markers.[21] We found the expression of CD69 and CD25 was significantly increased in *Phf6*^{R274X} T cells as compared to controls (Figures 2G and 2H). Furthermore, *Phf6*^{R274X} increased the expression of TNF-α,

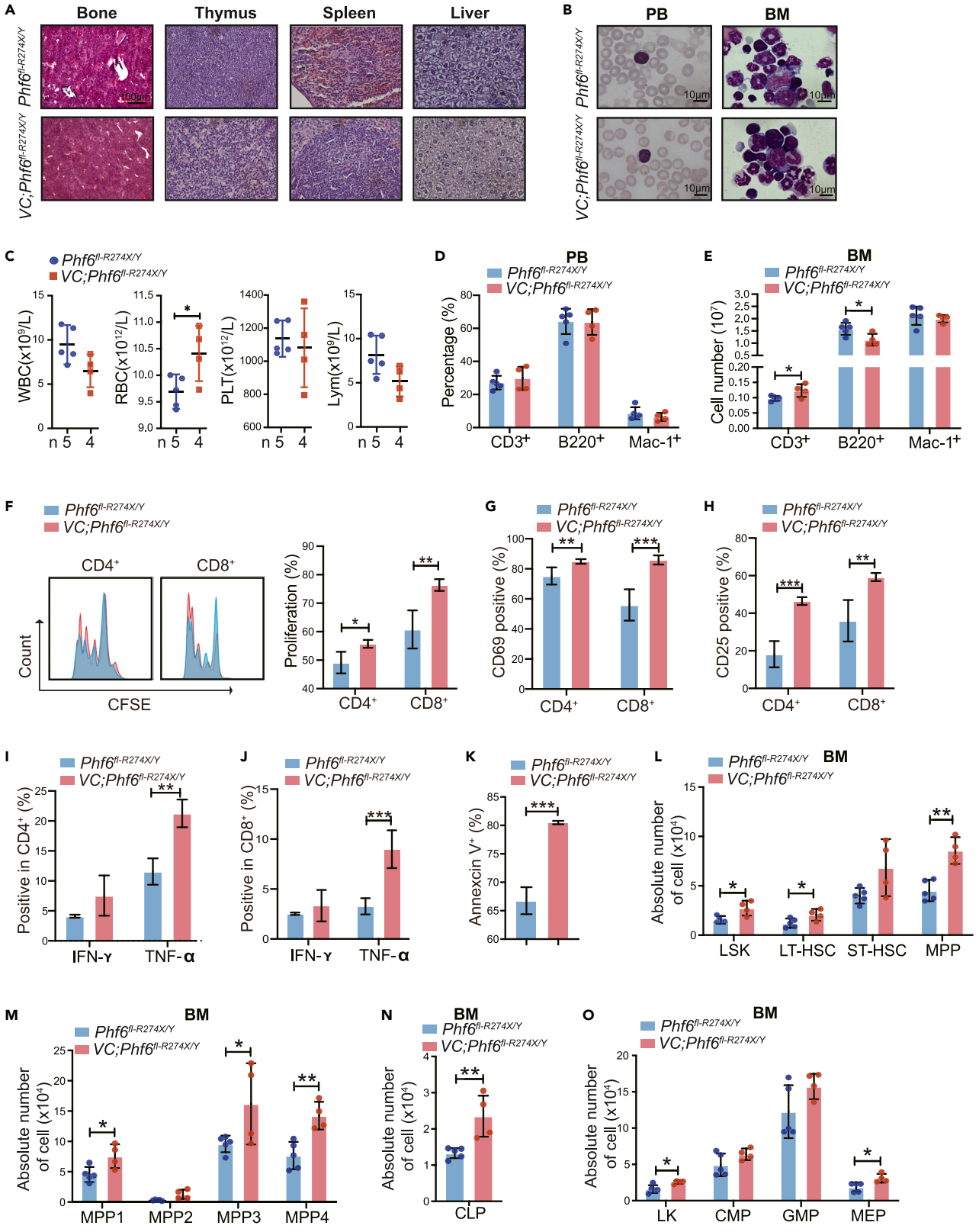
A
Bone
Thymus
Spleen
Liver
Phf6fl-R274X/Y
VC;Phf6fl-R274X/Y
100μm
B
PB
BM
10μm
C
WBC(x10⁹/L)
RBC(x10¹²/L)
PLT(x10¹²/L)
Lym(x10⁹/L)
n 5 4
D
PB
Percentage (%)
CD3⁺
B220⁺
Mac-1⁺
E
BM
Cell number (10⁷)
F
CD4⁺
CD8⁺
Count
CFSE
Proliferation (%)
G
CD69 positive (%)
H
CD25 positive (%)
I
Positive in CD4⁺ (%)
IFN-γ
TNF-α
J
Positive in CD8⁺ (%)
K
Annexin V⁺ (%)
L
BM
Absolute number of cell (x10⁴)
LSK
LT-HSC
ST-HSC
MPP
M
BM
MPP1
MPP2
MPP3
MPP4
N
BM
CLP
O
BM
LK
CMP
GMP
MEP

Figure 2. *Phf6*^{R274X} mutation increases the proliferation of hematopoietic stem cells

(A) Hematoxylin and eosin (H&E) staining of BM, spleen, thymus, and liver.

(B) Wright-Giemsa staining of PB smears and BM cytospin.

(C) White blood cell (WBC), red blood cell (RBC), platelet (PLT), and lymphocyte (Lym) counts in PB by routine blood tests from *Phf6*$^{fl\text{-}R274X/Y}$ (n = 5) and *Vav1-Cre;Phf6*$^{fl\text{-}R274X/Y}$ (n = 4).

(D) FACS analysis of the percentage of T, B and myeloid cells in PB and BM from *Phf6*$^{fl\text{-}R274X/Y}$ (n = 5) and *Vav1-Cre;Phf6*$^{fl\text{-}R274X/Y}$ (n = 4) mice.

(E) The absolute number of T, B, and myeloid cells in BM from *Phf6*$^{fl\text{-}R274X/Y}$ (n = 5) and *Vav1-Cre;Phf6*$^{fl\text{-}R274X/Y}$ (n = 4) mice.

(F) Primary T cells from *Phf6*$^{fl\text{-}R274X/Y}$ and *Vav1-Cre;Phf6*$^{fl\text{-}R274X/Y}$ mice were treated with anti-CD3/CD28 antibodies for 24 h. The proliferation index of CD4$^+$ and CD8$^+$ cells were measured by CFSE-staining analysis (n = 4).

(G and H) Primary T cells from *Phf6*$^{fl\text{-}R274X/Y}$ and *Vav1-Cre;Phf6*$^{fl\text{-}R274X/Y}$ mice were treated with anti-CD3/CD28 antibodies and analyzed by flow cytometry (n = 4). (G) Stimulated for 12h and expression of CD69 on both CD4$^+$ and CD8$^+$ T cells. (H) Stimulated for 72 h and expression of CD25 on both CD4$^+$ and CD8$^+$ T cells.

(I and J) After primary T cells were treated with anti-CD3/CD28 antibodies for 24 h, cells were stimulated with the indicated concentrations of PMA, ionomycin, and Golgiplug for 6h. Flow cytometric analysis of IFN-γ and TNF-α secretion by (I) CD4$^+$ cell; (J) CD8$^+$ cell (n = 3).

(K) Primary T cells from *Phf6*$^{fl\text{-}R274X/Y}$ and *Vav1-Cre;Phf6*$^{fl\text{-}R274X/Y}$ mice-mediated killing assay in primary spleen cells from MAL-AF9 mice, measured by Annexin V staining (n = 3).

(L–O) The absolute number of LSK (Lin$^-$Sca1$^+$c-Kit$^+$) cells, LT-HSC (Lin$^-$Sca1$^+$c-Kit$^+$CD34$^-$Flt3^{low}), ST-HSC (Lin$^-$Sca1$^+$c-Kit$^+$CD34$^+$Flt3^{low}), MPP (Lin$^-$Sca1$^+$c-Kit$^+$CD34$^+$Flt3$^+$), MPP1 (Lin$^-$c-Kit$^+$Sca1$^-$CD135$^-$CD150$^-$CD48$^-$), MPP2 (Lin$^-$c-Kit$^+$Sca1$^-$CD135$^-$CD150$^+$CD48$^+$), MPP3 (Lin$^-$c-Kit$^+$Sca1$^-$CD135$^-$CD150$^-$CD48$^+$), MPP4 (Lin$^-$c-Kit$^+$Sca1$^-$CD135$^+$CD150$^-$CD48$^+$), LK (Lin$^-$Sca1$^-$c-Kit$^+$) cells, CMP (Lin$^-$c-Kit$^+$Sca1$^-$CD34$^+$CD16/32^{low}), GMP (Lin$^-$c-Kit$^+$Sca1$^-$CD34$^+$CD16/32^{high}) and MEP (Lin$^-$c-Kit$^+$Sca1$^-$CD34$^-$CD16/32^{low}) populations, and CLP (Lin$^-$IL-7r$^+$Sca1$^+$c-Kit$^+$) in BM from *Phf6*$^{fl\text{-}R274X/Y}$ (n = 5) and *Vav1-Cre;Phf6*$^{fl\text{-}R274X/Y}$ (n = 4) mice. Data information: All mice used here were male mice of 8–10 weeks of age. In (C–O) data are shown as the mean ± SD. *p < 0.05, **p < 0.01, and ***p < 0.001 by the Student's *t* test.

while it did not alter IFN-γ production in CD4$^+$ and CD8$^+$ T cells (Figure 2IJ). It suggested that *Phf6*^{R274X} might promote the proliferation and activation of T cells. We, thus, further examined the role of *Phf6*^{R274X} in T cell functioning by measuring T cell-mediated killing after CD3$^+$ T cells were co-cultured with primary spleen cells from MLL-AF9-induced AML mouse model for 12 h. We found that *Phf6*^{R274X} mutation increased the killing abilities of T cells (Figure 2K). These results demonstrated that *Phf6*^{R274X} mutation might affect the function of T cells.

We further investigated the role of *Phf6*^{R274X} mutation in HSC/HPCs *in vivo*. We found that absolute number of LSK (Lin$^-$Sca-1$^+$c-Kit$^+$) cells, long term-HSCs (LT-HSCs), and Multipotent blood progenitors (MPP) was higher in the BM of *Vav1-Cre;Phf6*$^{fl\text{-}R274X/Y}$ mice than that of controls (Figure 2L). The cell count of MPP1, MPP3, and MPP4 was also increased in the BM of *Vav1-Cre;Phf6*$^{fl\text{-}R274X/Y}$ mice (Figure 2M). The absolute number of common lymphoid progenitor (CLP), LK (Lin$^-$Sca-1$^-$c-Kit$^+$), and megakaryocyte–erythroid progenitor cell (MEP) was increased in the BM of *Vav1-Cre;Phf6*$^{fl\text{-}R274X/Y}$ mice as compared with controls (Figures 2N and 2O). In addition, the percentage of LSK cells and LK cells were equivalent in spleen of Phf6^{R274X} mice and the control mice (Figure S2E and S2F). Collectively, these data indicated that *Phf6*^{R274X} mutation increased the HSC/HPC pool *in vivo*.

Phf6^{R274X} mutation increases HSCs regeneration ability and skews differentiation toward T cells in competitive transplantation assay

To further probe the potential role of *Phf6*^{R274X} mutation in regulating the function of HSCs, we performed serial competitive transplantations assay. We transplanted BM cells from *Phf6*$^{fl\text{-}R274X/Y}$ *or Vav1-Cre;Phf6*$^{fl\text{-}R274X/Y}$ CD45.2$^+$ mice together with CD45.1$^+$ BM cells into lethally irradiated CD45.1$^+$ recipient mice (Figure 3A). Every four months after each transplantation, we performed flow cytometric assay to examine the frequency of reconstituted cells (CD45.2$^+$) in PB. The chimerism of *Vav1-Cre;Phf6*$^{fl\text{-}R274X/Y}$ cells (CD45.2$^+$) in PB was significantly higher than that of the control in primary (1°) and secondary (2°) transplantations (Figure 3B). Notably, the percentage of donor-derived cells (CD45.2$^+$) in CD3$^+$ T cells was increased in the PB from the mice transplanted with *Vav1-Cre;Phf6*$^{fl\text{-}R274X/Y}$ BM cells (Figure 3C). We also found that the weight of thymus was significantly higher in *Vav-Cre1;Phf6*$^{fl\text{-}R274X/Y}$ group than the controls in the 1° and 2° transplantations (Figure 3D, S3A), and the percentage of donor-derived cells (CD45.2$^+$) were significantly increased in thymus of mice transplanted with *Vav1-Cre;Phf6*$^{fl\text{-}R274X/Y}$ cells (Figure 3E). The absolute number of BM cells in mice transplanted with *Vav-Cre1;Phf6*$^{fl\text{-}R274X/Y}$ BM cells was equivalent to that of the controls in 1° and 2° transplantations (Figure 3F, S3B). The percentage of donor-derived cells (CD45.2$^+$) were significantly increased in BM of mice transplanted with *Vav1-Cre;Phf6*$^{fl\text{-}R274X/Y}$ cells when compared with that of the controls in primary (1°) and secondary (2°) transplantations (Figure 3G, S3C). Consistent with CD45.2$^+$ T cells in PB, the percentage of donor-derived

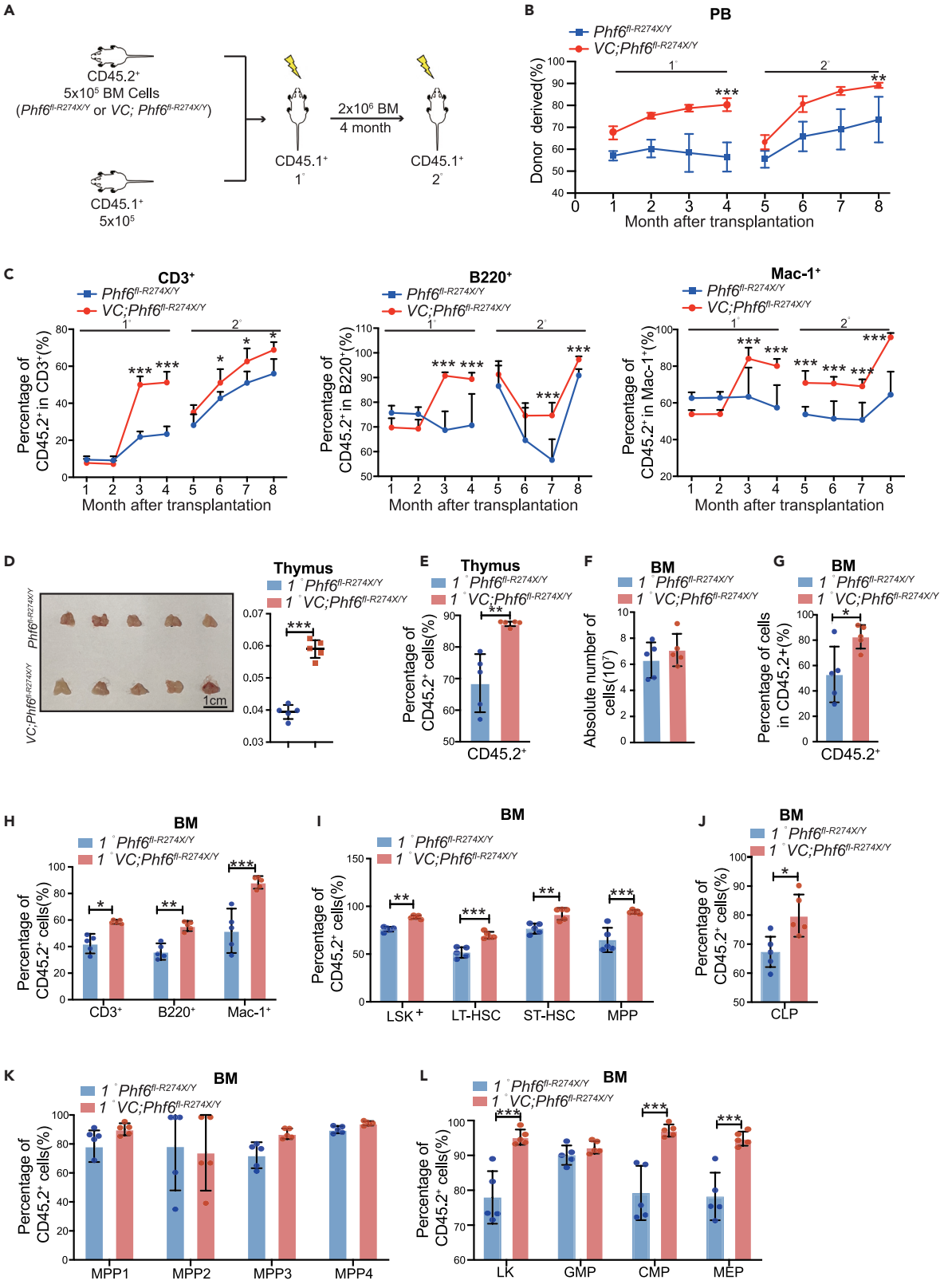
A
CD45.2+
5x10^5 BM Cells
(Phf6fl-R274X/Y or VC; Phf6fl-R274X/Y)
CD45.1+
5x10^5
CD45.1+
1°
2x10^6 BM
4 month
CD45.1+
2°
B
PB
Phf6fl-R274X/Y
VC;Phf6fl-R274X/Y
Donor derived(%)
Month after transplantation
C
CD3+
B220+
Mac-1+
Percentage of CD45.2+ in CD3+(%)
Percentage of CD45.2+ in B220+(%)
Percentage of CD45.2+ in Mac-1+(%)
Month after transplantation
D
Thymus
1cm
E
Thymus
Percentage of CD45.2+ cells(%)
CD45.2+
F
BM
Absolute number of cells(10^7)
G
BM
Percentage of cells in CD45.2+(%)
CD45.2+
H
BM
Percentage of CD45.2+ cells(%)
CD3+
B220+
Mac-1+
I
BM
Percentage of CD45.2+ cells(%)
LSK+
LT-HSC
ST-HSC
MPP
J
BM
Percentage of CD45.2+ cells(%)
CLP
K
BM
Percentage of CD45.2+ cells(%)
MPP1
MPP2
MPP3
MPP4
L
BM
Percentage of CD45.2+ cells(%)
LK
GMP
CMP
MEP

Figure 3. *Phf6*^{R274X} mutation enhanced competitive hematopoietic reconstitution

(A) Schematic diagram showing the experimental design for serial competitive hematopoietic transplantation with BM cells from *Phf6*$^{fl\text{-}R274X/Y}$ and *Vav1-Cre;Phf6*$^{fl\text{-}R274X/Y}$ mice.

(B) The chimerism of donor-derived cell (CD45.2$^+$) in PB of primary (1°) and secondary (2°) recipients (n = 5).

(C) The chimerism of donor-derived T, B, and myeloid cells in PB of primary (1°) and secondary (2°) recipients (n = 5).

(D) Photographs and weight of thymus of primary (1°) recipients at 4 months after transplantation (n = 5).

(E) The chimerism of donor-derived cell in thymus of primary (1°) recipients at fourth month after transplantation (n = 5).

(F) Absolute number of BM cells in primary (1°) recipients (n = 6). (G-L) The chimerism of donor-derived cell in BM of primary (1°) recipients at fourth month after transplantation (n = 6).

(G–L) (G) donor-derived cells (CD45.2$^+$), (H) donor-derived T, B, and myeloid cells, (I) donor-derived LKS, LT-HSC, ST-HSC, and MPP cells, (J) donor-derived CLP, (K) donor-derived MPP1-4, (L) donor-derived LK, GMP, CMP, MEP. Data information: All mice for donor cells used were male mice of 8–10 weeks of age. In (B-L) data are shown as the mean ± SD. *p < 0.05, **p < 0.01, and ***p < 0.001 by the Student's *t* test.

cells (CD45.2$^+$) in CD3$^+$ T cells were also increased in BM of *Vav1-Cre;Phf6*$^{fl\text{-}R274X/Y}$ recipients in 1° and 2° transplantations (Figures 3G–3I, S3D–S3F), indicating that the differentiation of *Phf6*^{R274X} HSCs biased toward T cells. Interestingly, in LT-HSC/HPC fractions, the percentage of *Vav1-Cre;Phf6*$^{fl\text{-}R274X/Y}$ derived cells in LSKs, LT-HSC, short term-HSC (ST-HSC), MPP, LKs, common-myeloid progenitors (CMP), MEP, and CLP was much higher than that of control in 1° transplantation (Figure 3J, S3G), suggesting that *Phf6*^{R274X} increased the self-renewal ability of HSCs. Taken together, these results indicated that *Phf6*^{R274X} mutation led to increase the hematopoietic reconstitution and skewed HSCs toward T cells differentiation.

Phf6^{R274X} mutation in HSCs lead to a distinct gene expression signature associated with cell proliferation and differentiation

To determine the underlying mechanism of *Phf6*^{R274X} in regulating the function of HSC/HPCs, we performed RNA sequencing and analyzed the different expression profiles between Phf6^{R274X} LSK cells and controls. Consistent with *Phf6*^{R274X}-induced over-activation of HSCs *in vivo*, the different expression genes (DEGs) were enriched in cell viability-related signaling pathways, such as cell activation, adhesion, and leukocyte differentiation (Figure 4A). Furthermore, DEGs were also enriched in cancer-related pathways, such as cytokine-cytokine receptor interaction, transcription factor activity, and positive regulation of MAPK cascade and transcription dysregulation (Figure 4A), suggesting *Phf6*^{R274X} might involve in tumorigenesis. The expression profiles of *Phf6*^{R274X} LSK cells showed 66 genes related to leukocyte proliferation and differentiation were upregulated (p < 0.05) (Figure 4B). Gene set enrichment analysis (GSEA) showed that the upregulated genes in *Phf6*^{R274X} LSK cells were enriched in GRAHAM_NORMAL_QUIESCENT_VS._NORMAL_DIVIDING_DN and GAL_LEUKEMIC_STEM_CELL_DN pathway, as well as T cell in proliferation and differentiation (Figure 4C). Gene ontology (GO) analysis revealed that the upregulated genes in *Phf6*^{R274X} LSK cells were associated with T cell activation, lymphocyte proliferation, and T cell differentiation (Figure 4D). Kyoto Encylopaedia of Genes and Genomes (KEGG) analysis revealed active cytokine-cytokine receptor interaction pathway (Figure 4E). Interestingly, the genes related to the regulation of HSC function, such as *Vdr* and *Itga2b* were significantly downregulated, while *Abcc3* was upregulated in *Phf6*^{R274X} group (Figure 4F). The profiles derived from analyses were consistent with the experimental findings that *Phf6*^{R274X} mutation enhanced the regeneration capacity of HSC. In addition, the mRNA expression of *CD3e*, *Igf1*, *Xbp1, and Aif1*, that were involved in T cell proliferation and differentiation, were increased in *Phf6*^{R274X} LSK cells (Figure 4G), which further supported that *Phf6*^{R274X} mutation activated the function of T cell.

DISCUSSION

Phf6 is an important epigenetic regulatory gene, and its significance was anchored by clinical findings that numerous mutations were found in leukemia patients. However, current findings are mainly from studies using Phf6 deletion mutation mouse models. For example, Wendorff and Miyagi et al. demonstrated that Phf6 deletion increased the self-renewal ability of HSCs.[8,9] As one of the most common mutation identified in both T-ALL and AML patients, the consequence of *PHF6*^{R274X} mutation in the hematopoietic system are still largely unknown. In the current study, we generated a *Phf6*^{R274X} knock-in mouse model which expressed Phf6^{R274X} in the hematopoietic compartment. Consistent with Phf6-deficient mice in previous studies,[6–8] *VC;Phf6*$^{fl\text{-}R274X/Y}$ mice displayed an increase of HSCs pool in BM and enhanced self-renewal ability of LT-HSCs when compared to the control. This result suggests that *VC;Phf6*$^{fl\text{-}R274X/Y}$ mice showed the phenotypes resembling Phf6 null mice. In contrast, the differentiation of *Phf6*^{R274X} HSCs skewed toward

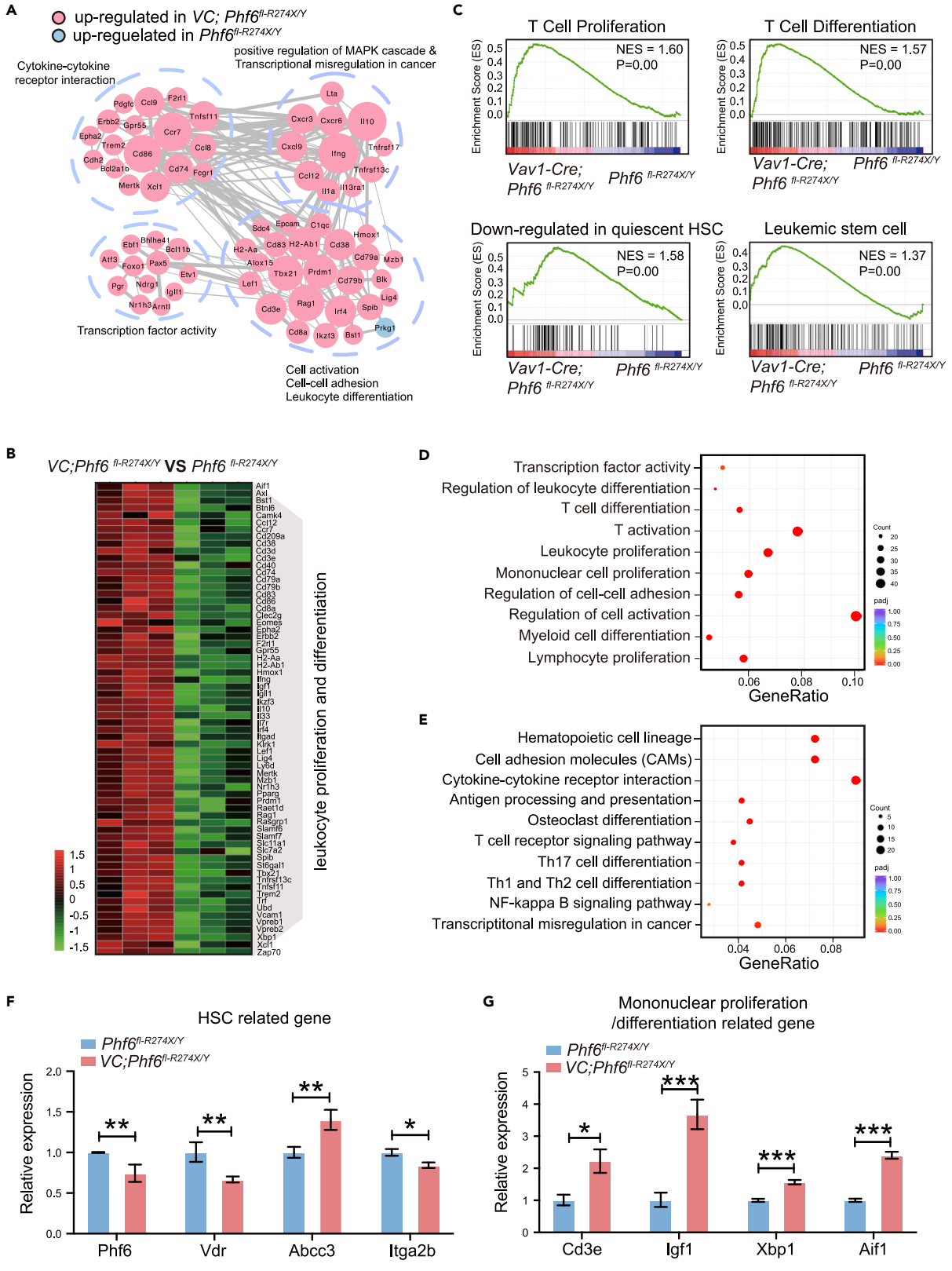
A
up-regulated in VC; Phf6fl-R274X/Y
up-reguelated in Phf6fl-R274X/Y
positive regulation of MAPK cascade &
Transcriptional misregulation in cancer
Cytokine-cytokine
receptor interaction
Transcription factor activity
Cell activation
Cell-cell adhesion
Leukocyte differentiation
C
T Cell Proliferation
NES = 1.60
P=0.00
T Cell Differentiation
NES = 1.57
P=0.00
Down-regulated in quiescent HSC
NES = 1.58
P=0.00
Leukemic stem cell
NES = 1.37
P=0.00
Enrichment Score (ES)
Vav1-Cre;
Phf6 fl-R274X/Y
B
VC;Phf6 fl-R274X/Y VS Phf6 fl-R274X/Y
leukocyte proliferation and differentiation
D
Transcription factor activity
Regulation of leukocyte differentiation
T cell differentiation
T activation
Leukocyte proliferation
Mononuclear cell proliferation
Regulation of cell-cell adhesion
Regulation of cell activation
Myeloid cell differentiation
Lymphocyte proliferation
GeneRatio
Count
padj
E
Hematopoietic cell lineage
Cell adhesion molecules (CAMs)
Cytokine-cytokine receptor interaction
Antigen processing and presentation
Osteoclast differentiation
T cell receptor signaling pathway
Th17 cell differentiation
Th1 and Th2 cell differentiation
NF-kappa B signaling pathway
Transcriptitonal misregulation in cancer
GeneRatio
F
HSC related gene
Phf6fl-R274X/Y
VC;Phf6fl-R274X/Y
Relative expression
Phf6
Vdr
Abcc3
Itga2b
G
Mononuclear proliferation
/differentiation related gene
Cd3e
Igf1
Xbp1
Aif1

Figure 4. *Phf6*^{R274X} mutation alters the gene expression profiles in HSC/HPCs

(A) Gene interaction analysis showing the significantly altered expression pattern in *Vav1-Cre;Phf6*$^{fl\text{-}R274X/Y}$ BM LSK^{+} cells compared with control cells.

(B) Heatmap showing differential expression of 66 genes related to leukocyte proliferation and differentiation in *Phf6*$^{fl\text{-}R274X/Y}$ and *Vav1-Cre;Phf6*$^{fl\text{-}R274X/Y}$ mice BM LSK^{+} cells. |Log2foldchange | > 1, p value <0.05 (n = 3).

(C) Gene set enrichment analysis (GSEA) for genes affected in the BM LSK^{+} cell from *Phf6*$^{fl\text{-}R274X/Y}$ and *Vav1-Cre;Phf6*$^{fl\text{-}R274X/Y}$ mice.

(D and E) GO and KEGG analysis of the up-regulated genes in *Vav1-Cre;Phf6*$^{fl\text{-}R274X/Y}$ cells compared with *Phf6*$^{fl\text{-}R274X/Y}$ cells.

(F and G) Relative expression levels of Aif1, Cd3e, Igf1, and Xbp1 genes in BM LSK^{+} cells from *Phf6*$^{fl\text{-}R274X/Y}$ and *Vav1-Cre;Phf6*$^{fl\text{-}R274X/Y}$ mice. mRNA levels were normalized to the expression of GAPDH. Data information: in (F-G) data are shown as the mean ± SD. *p < 0.05, **p < 0.01, and ***p < 0.001 by the Student's *t* test.

T cells and *Phf6*^{R274X} enhanced the activity of T cell activation, proliferation, and killing. This T cell phenotype was specific to *VC;Phf6*$^{fl\text{-}R274X/Y}$ mice, indicating that PHF6^{R274X} mutation has a unique role in T cell lineage differentiation and function, and further studies maybe needed. The changes in RBCs and B cells might be temporary for *Phf6*^{R274X} mice. These data demonstrated that the function of *Phf6*^{R274X} in hematopoiesis is altered.

PHF6^{R274X} mutation frequently occurred in T-ALL and AML patients, suggesting that *PHF6*^{R274X} might involve in leukemogenesis of AML and T-ALL. Several studies indicated that PHF6 functions as a tumor suppressor in T-ALL. For example, Wendorff and Yuan et al. observed that Phf6 loss promoted T-ALLs driven by ICN1 and JAK3 mutation.[8,22] In contrast to tumor suppressing role seen in PHF6 in T-ALL, Phf6 deficiency was shown to inhibit the progression of BCR-ABL-induced B-ALL *in vivo*, indicated that Phf6 might possess an oncogenic role in B-ALL[11]. In this context, we found that *Phf6*^{R274X} mice did not develop hematological malignancies spontaneously. RNA-Seq analysis showed more active transcriptome programming in *Phf6*^{R274X} LSK cells when compared to controls. Gene expression profiling implicated in cell activation, cell-cell adhesion, and cell differentiation of *Phf6*^{R274X} LSK cells, supporting the findings of *Phf6*^{R274X} in HSC homeostasis. We also found that GEGs were enriched in genes related to leukemia stem cell (LSC), as LSC and normal HSC have been shown to share some common molecular mechanisms previously.[23,24] Of these enriched genes, we found that *Vdr, Abcc3,* and *Itga2b* were also dysregulated in *Phf6*^{R274X} mutant LSKs. It has been reported that *Vdr, Itga2b,* and *Abcc3* directly regulated the function of HSCs.[25–27] For example, Ewa Marcinkowska., et al. found that vitamin D receptor (VDR) is present in multiple types of blood cells. While the expression of VDR was silenced during differentiation of HSCs.[26] Jon Frampton., et al. found that the product of the Itga2b gene, CD41 contributes to the function of HSCs. The expression of Itga2b (CD41) was negative during the onset of definitive hematopoiesis.[25] In addition, Chi Wai Eric So., et al. found that patients with HSC-like AML had higher expression of ABCC3. Knockdown of ABCC3 by two independent shRNAs inhibited the survival of MLL-rearranged HSCs.[27] Moreover, D Givol1., et al. found that some of the "signature" genes of LSC are alike within the cell stage of HSCs[28] including these three genes that were enriched in GAL_LEUKEMIC_STEM_CELL_DN pathway by our analysis. Thus, we speculated that these three genes share some expression similarities in LSC and HSC, although more functional studies are needed. It also implicated that Phf6^{R274X} may affect the function of HSCs and play a role in leukemia. In this regard, *Phf6*^{R274X} seemed to enhance the self-renewal capacity of HSCs, potentially to play roles in leukemia development. In addition, a set of genes (*Aif1*, *Cd3e*, *Igf1*, and *Xbp1*) associated with T cells activation were upregulated in the *Phf6*^{R274X} mutation group, which might partially explain *Phf6*^{R274X} promoted the function of T cells. The transcriptional regulation of T cells development via lineage-specific factors has been well characterized.[29] Previous study found that PHF6 binds to nucleosomes surrounding the TSSs of T-cell-specific genes, coordinating chromatin compaction, and blocking the binding of T cell-specific transcription factors.[30] Thus, chromatin regions that became more accessible upon Phf6 mutation (or loss) could be enriched for motifs of transcription factors associated with the development of T-ALL. In view of this, we speculated that chromatin binding for T cell-specific TFs is more accessible due to *Phf6*^{R274X} mutation, and T cell-specific transcription factors might bind and activate the transcriptome programming in LSK cells, and the up-regulated genes that involved in T cell proliferation and differentiation, ultimately led to the expansion of lymphoid-primed progenitor cells.

PHF6^{R274X} is located on the ePHD2 domain and is essential for the function of PHF6,[2,15] and we are particularly interested in the effect of R274X mutation on protein level since it is a nonsense mutation. We determined that the mRNA level of *Phf6*^{R274X} was significantly decreased in *Phf6*^{R274X}-mutated mice (Figure 1F). Moreover, we found that the degradation of Phf6^{R274X} mRNA was faster than wild-type Phf6 mRNA in BM cells following Actinomycin-D (10 μg/mL) treatment (data not shown). It indicated that although *Phf6*^{R274X} gene could successfully be transcribed to mRNA, the stability of Phf6^{R274X} mRNA was reduced. Since the

nonsense-mediated decay (NMD) is a known cellular mechanism designed to degrade mRNAs to control proper levels of gene expression by removing mRNAs that potentially encode deleterious truncated proteins,[31,32] we speculated that the R274X mutation rendered its mRNA unstable, less mutant protein is synthesized or if synthesized, be degraded due to its structure instability, and the function of protein was further impaired. The phenotype discrepancies seen between the Phf6 knockout mice and *Phf6*^{R274X} knock-in mice may lies in this, and further studies is needed to fully elucidate the regulatory role of PHF6 in hematopoiesis. In conclusion, we found that *Phf6*^{R274X} mutation frequently existed in T-ALL and AML patients. Notably, *Phf6*^{R274X} mutation results in increased self-renewal of HSCs and skewed differentiation to T cells *in vivo*. The *Phf6*^{R274X} mice is a suitable mouse model for further studies in the physiology/pathophysiology of hematopoiesis and leukemia and the molecular pathways regulated by *Phf6* mutations.

Limitations of study

Here in this study, we generated a *Phf6*^{R274X} knock-in mouse model to elucidate the effect of *Phf6*^{R274X} mutation in hematopoiesis *in vivo*. While we demonstrated that *Phf6*^{R274X} mutation promoted self-renewal ability of HSCs and T cells proliferation and activation, the underlying mechanism remains to be elucidated. Our data suggested that the phenotypes of *Phf6*^{R274X} mice and Phf6-deficient mice have both similarities and differences, suggesting a differential role of Phf6^{R274X} mutation. Further work is needed to explore the potential role of *PHF6*^{R274X} mutation in leukemia progression.

STAR★METHODS

Detailed methods are provided in the online version of this paper and include the following:

- KEY RESOURCES TABLE
- RESOURCE AVAILABILITY
  - Lead contact
  - Materials availability
  - Data and code availability
- EXPERIMENTAL MODEL AND SUBJECT DETAILS
  - Mice
- METHOD DETAILS
  - Real time PCR
  - Western blotting analysis
  - Bone marrow transplantation
  - Flow cytometry
  - T cell isolation and culture
  - Detection of CD69 and CD25 expression
  - CFSE staining
  - Intracellular cytokine staining
  - T cell killing assay
  - RNA sequencing
- QUANTIFICATION AND STATISTICAL ANALYSIS

SUPPLEMENTAL INFORMATION

Supplemental information can be found online at https://doi.org/10.1016/j.isci.2023.106817.

ACKNOWLEDGMENTS

This work was supported by funds from the National Key Research and Development Program of China (2020YFE0203000 to YJC), the National Natural Science Foundation of China (82270153, 82070169 to XMW), and the Chinese Academy of Medical Sciences Innovation Fund for Medical Sciences, CIFMS (2021-I2M-1-040 to WPY). Haihe Laboratory of Cell Ecosystem Innovation Fund (22HHXBSS00037 to WPY, YJC and YGC).

AUTHOR CONTRIBUTIONS

X.M.W. and W.P.Y. conceived the project, supervised the research, and revised the paper. Y.J.L., S.N.Y., and T.X.G. performed most of the experiments, analyzed the data, and wrote the manuscript. T.X.G., S.B.H., F.Z., W.Z.Y., and Y.G.C. assisted with the mouse experiments, flow cytometry analysis, and data

processing. Y.J.C. and E.L.J. participated in results and paper discussion. All authors have read and approved the final manuscript.

DECLARATION OF INTERESTS

The authors declare no conflict of interest.

INCLUSION AND DIVERSITY

We support inclusive, diverse, and equitable conduct of research.

Received: August 11, 2022
Revised: February 25, 2023
Accepted: May 2, 2023
Published: May 5, 2023

REFERENCES

1. Landais, S., Quantin, R., and Rassart, E. (2005). Radiation leukemia virus common integration at the Kis2 locus: simultaneous overexpression of a novel noncoding RNA and of the proximal Phf6 gene. J. Virol. *79*, 11443–11456.

2. Liu, Z., Li, F., Ruan, K., Zhang, J., Mei, Y., Wu, J., and Shi, Y. (2014). Structural and functional insights into the human Börjeson-Forssman-Lehmann syndrome-associated protein PHF6. J. Biol. Chem. *289*, 10069–10083.

3. Aasland, R., Gibson, T.J., and Stewart, A.F. (1995). The PHD finger: implications for chromatin-mediated transcriptional regulation. Trends Biochem. Sci. *20*, 56–59.

4. Wang, J., Leung, J.W.c., Gong, Z., Feng, L., Shi, X., and Chen, J. (2013). PHF6 regulates cell cycle progression by suppressing ribosomal RNA synthesis. J. Biol. Chem. *288*, 3174–3183.

5. Loontiens, S., Dolens, A.C., Strubbe, S., Van de Walle, I., Moore, F.E., Depestel, L., Vanhauwaert, S., Matthijssens, F., Langenau, D.M., Speleman, F., et al. (2020). PHF6 expression levels impact human hematopoietic stem cell differentiation. Front. Cell Dev. Biol. *8*, 599472.

6. Hsu, Y.C., Chen, T.C., Lin, C.C., Yuan, C.T., Hsu, C.L., Hou, H.A., Kao, C.J., Chuang, P.H., Chen, Y.R., Chou, W.C., and Tien, H.F. (2019). Phf6-null hematopoietic stem cells have enhanced self-renewal capacity and oncogenic potentials. Blood Adv. *3*, 2355–2367.

7. McRae, H.M., Garnham, A.L., Hu, Y., Witkowski, M.T., Corbett, M.A., Dixon, M.P., May, R.E., Sheikh, B.N., Chiang, W., Kueh, A.J., et al. (2019). PHF6 regulates hematopoietic stem and progenitor cells and its loss synergizes with expression of TLX3 to cause leukemia. Blood *133*, 1729–1741.

8. Miyagi, S., Sroczynska, P., Kato, Y., Nakajima-Takagi, Y., Oshima, M., Rizq, O., Takayama, N., Saraya, A., Mizuno, S., Sugiyama, F., et al. (2019). The chromatin-binding protein Phf6 restricts the self-renewal of hematopoietic stem cells. Blood *133*, 2495–2506.

9. Wendorff, A.A., Quinn, S.A., Rashkovan, M., Madubata, C.J., Ambesi-Impiombato, A., Litzow, M.R., Tallman, M.S., Paietta, E., Paganin, M., Basso, G., et al. (2019). Phf6 loss enhances HSC self-renewal driving tumor initiation and leukemia stem cell activity in T-ALL. Cancer Discov. *9*, 436–451.

10. Loontiens, S., Vanhauwaert, S., Depestel, L., Dewyn, G., Van Loocke, W., Moore, F.E., Garcia, E.G., Batchelor, L., Borga, C., Squiban, B., et al. (2020). A novel TLX1-driven T-ALL zebrafish model: comparative genomic analysis with other leukemia models. Leukemia *34*, 3398–3403.

11. Meacham, C.E., Lawton, L.N., Soto-Feliciano, Y.M., Pritchard, J.R., Joughin, B.A., Ehrenberger, T., Fenouille, N., Zuber, J., Williams, R.T., Young, R.A., and Hemann, M.T. (2015). A genome-scale in vivo loss-of-function screen identifies Phf6 as a lineage-specific regulator of leukemia cell growth. Genes Dev. *29*, 483–488.

12. Van Vlierberghe, P., Palomero, T., Khiabanian, H., Van der Meulen, J., Castillo, M., Van Roy, N., De Moerloose, B., Philippé, J., González-García, S., Toribio, M.L., et al. (2010). PHF6 mutations in T-cell acute lymphoblastic leukemia. Nat. Genet. *42*, 338–342.

13. Van Vlierberghe, P., Patel, J., Abdel-Wahab, O., Lobry, C., Hedvat, C.V., Balbin, M., Nicolas, C., Payer, A.R., Fernandez, H.F., Tallman, M.S., et al. (2011). PHF6 mutations in adult acute myeloid leukemia. Leukemia *25*, 130–134.

14. Mori, T., Nagata, Y., Makishima, H., Sanada, M., Shiozawa, Y., Kon, A., Yoshizato, T., Sato-Otsubo, A., Kataoka, K., Shiraishi, Y., et al. (2016). Somatic PHF6 mutations in 1760 cases with various myeloid neoplasms. Leukemia *30*, 2270–2273.

15. Liu, Z., Li, F., Ruan, K., Zhang, J., Mei, Y., Wu, J., and Shi, Y. (2014). Structural and functional insights into the human Borjeson-Forssman-Lehmann syndrome-associated protein PHF6. J. Biol. Chem. *289*, 10069–10083.

16. Wang, Q., Qiu, H., Jiang, H., Wu, L., Dong, S., Pan, J., Wang, W., Ping, N., Xia, J., Sun, A., et al. (2011). Mutations of PHF6 are associated with mutations of NOTCH1, JAK1 and rearrangement of SET-NUP214 in T-cell acute lymphoblastic leukemia. Haematologica *96*, 1808–1814.

17. Grossmann, V., Haferlach, C., Weissmann, S., Roller, A., Schindela, S., Poetzinger, F., Stadler, K., Bellos, F., Kern, W., Haferlach, T., et al. (2013). The molecular profile of adult T-cell acute lymphoblastic leukemia: mutations in RUNX1 and DNMT3A are associated with poor prognosis in T-ALL. Genes Chromosomes Cancer *52*, 410–422.

18. Huh, H.J., Lee, S.H., Yoo, K.H., Sung, K.W., Koo, H.H., Jang, J.H., Kim, K., Kim, S.J., Kim, W.S., Jung, C.W., et al. (2013). Gene mutation profiles and prognostic implications in Korean patients with T-lymphoblastic leukemia. Ann. Hematol. *92*, 635–644.

19. Li, M., Xiao, L., Xu, J., Zhang, R., Guo, J., Olson, J., Wu, Y., Li, J., Song, C., and Ge, Z. (2016). Co-existence of PHF6 and NOTCH1 mutations in adult T-cell acute lymphoblastic leukemia. Oncol. Lett. *12*, 16–22.

20. Todd, M.A.M., Ivanochko, D., and Picketts, D.J. (2015). PHF6 Degrees of separation: the Multifaceted roles of a chromatin Adaptor protein. Genes *6*, 325–352.

21. Caruso, A., Licenziati, S., Corulli, M., Canaris, A.D., De Francesco, M.A., Fiorentini, S., Peroni, L., Fallacara, F., Dima, F., Balsari, A., and Turano, A. (1997). Flow cytometric analysis of activation markers on stimulated T cells and their correlation with cell proliferation. Cytometry *27*, 71–76.

22. Yuan, S., Wang, X., Hou, S., Guo, T., Lan, Y., Yang, S., Zhao, F., Gao, J., Wang, Y., Chu, Y., et al. (2021). PHF6 and JAK3 mutations cooperate to drive T-cell acute lymphoblastic leukemia progression. Leukemia *36*, 370–382.

23. Reya, T., Morrison, S.J., Clarke, M.F., and Weissman, I.L. (2001). Stem cells, cancer, and cancer stem cells. Nature *414*, 105–111.

24. Park, I.K., Qian, D., Kiel, M., Becker, M.W., Pihalja, M., Weissman, I.L., Morrison, S.J., and Clarke, M.F. (2003). Bmi-1 is required for maintenance of adult self-renewing haematopoietic stem cells. Nature *423*, 302–305.

25. Dumon, S., Walton, D.S., Volpe, G., Wilson, N., Dassé, E., Del Pozzo, W., Landry, J.R., Turner, B., O'Neill, L.P., Göttgens, B., and Frampton, J. (2012). Itga2b regulation at the onset of definitive hematopoiesis and commitment to differentiation. PLoS One *7*, e43300.

26. Nowak, U., Janik, S., Marchwicka, A., Łaszkiewicz, A., Jakuszak, A., Cebrat, M., and Marcinkowska, E. (2020). Investigating the role of Methylation in silencing of VDR gene expression in normal cells during hematopoiesis and in their leukemic counterparts. Cells *9*, 1991.

27. Zeisig, B.B., Fung, T.K., Zarowiecki, M., Tsai, C.T., Luo, H., Stanojevic, B., Lynn, C., Leung, A.Y.H., Zuna, J., Zaliova, M., et al. (2021). Functional reconstruction of human AML reveals stem cell origin and vulnerability of treatment-resistant MLL-rearranged leukemia. Sci. Transl. Med. *13*, eabc4822.

28. Gal, H., Amariglio, N., Trakhtenbrot, L., Jacob-Hirsh, J., Margalit, O., Avigdor, A., Nagler, A., Tavor, S., Ein-Dor, L., Lapidot, T., et al. (2006). Gene expression profiles of AML derived stem cells; similarity to hematopoietic stem cells. Leukemia *20*, 2147–2154.

29. Mullighan, C.G., Goorha, S., Radtke, I., Miller, C.B., Coustan-Smith, E., Dalton, J.D., Girtman, K., Mathew, S., Ma, J., Pounds, S.B., et al. (2007). Genome-wide analysis of genetic alterations in acute lymphoblastic leukaemia. Nature *446*, 758–764.

30. Soto-Feliciano, Y.M., Bartlebaugh, J.M.E., Liu, Y., Sánchez-Rivera, F.J., Bhutkar, A., Weintraub, A.S., Buenrostro, J.D., Cheng, C.S., Regev, A., Jacks, T.E., et al. (2017). PHF6 regulates phenotypic plasticity through chromatin organization within lineage-specific genes. Genes Dev. *31*, 973–989.

31. Popp, M.W.L., and Maquat, L.E. (2013). Organizing principles of mammalian nonsense-mediated mRNA decay. Annu. Rev. Genet. *47*, 139–165.

32. Ahmed, R., Sarwar, S., Hu, J., Cardin, V., Qiu, L.R., Zapata, G., Vandeleur, L., Yan, K., Lerch, J.P., Corbett, M.A., et al. (2021). Transgenic mice with an R342X mutation in Phf6 display clinical features of Börjeson-Forssman-Lehmann Syndrome (BFLS). Hum. Mol. Genet. *30*, 575–594.

STAR★METHODS

KEY RESOURCES TABLE

REAGENT or RESOURCE	SOURCE	IDENTIFIER
Antibodies		
Anti-Rabbit monoclonalAnti-PHF6	Sigma	Cat# HPA001023; RRID: AB_1079606
Anti-Rabbit monoclonal anti-GAPDH	Cell Signaling Technology	Cat#: CST2118
Anti-mouse CD45.1 (APC)	Invitrogen	Cat#: 17-0453-82; RRID: AB_469398
Anti-mouse CD45.1 (APC-Cy7)	Biolegend	Cat#: 560579
Anti-mouse CD45.1 (Percp-Cy5.5)	Invitrogen	Cat#: 45-0453-82
Anti-mouse CD45.2 (PE)	eBioscience	Cat#: 12-0454-83; RRID: AB_465679
Anti-mouse CD45.2 (Percp-Cy5.5)	eBioscience	Cat#: 45-0453-82; RRID: AB_953590
Anti-mouse CD3 (PE)	eBioscience	Cat#: 12-0454-83; RRID: AB_465679
Anti-mouse CD3 (FITC)	Biolegend	Cat#: 100204
Anti-mouse CD3 (Biotin)	Invitrogen	Cat#: 13-0032-82; RRID: AB_2572762
Anti-mouse CD11b (Mac-1) (APC-Cy7)	Biolegend	Cat#: 101226
Anti-mouse CD11b (Mac-1) (Alexa Fluor780)	Invitrogen	Cat#: 47-0112-82; RRID: AB_1603193
Anti-mouse B220 (CD45R) (PerCP-Cyanine5.5)	eBioscience	Cat#: 45-0452-82; RRID: AB_1107006
Anti-mouse B220 (CD45R) (Biotin)	eBioscience	Cat#: 36-0452-85; RRID: AB_469753
Anti-mouse CD135 (Flk2) (PE)	eBioscience	Cat#: 12-1351-82
Anti-mouse Ly-6G (Gr-1) (Biotin)	eBioscience	Cat#: 13-5931-85; RRID: AB_466801
Anti-mouse CD34 (FITC)	Invitrogen	Cat#: 11-0341-82; RRID: AB_465021
Anti-mouse Ter119 (Biotin)	Invitrogen	Cat#: 13-5921-85; RRID: AB_466798
Anti-mouse CD16/32 (APC)	eBioscience	Cat#: 17-0161-82; RRID: AB_469356
Anti-mouse CD16/32 (FITC)	eBioscience	Cat#: 11-0161-82; RRID: AB_464956
Anti-mouse CD127 (IL-7R) (PE)	Invitrogen	Cat#: 12-1271-82
Anti-mouse CD44 (PE)	eBioscience	Cat#: 12-0441-82; RRID: AB_465664
Anti-mouse CD4 (PE-Cy7)	eBioscience	Cat#: 25-0041-82; RRID: AB_469576
Anti-mouse CD4 (Biotin)	eBioscience	Cat#: 13-0043-85; RRID: AB_466334
Anti-mouse CD8a (APC)	Biolegend	Cat#: 100712
Anti-mouse CD8a (Biotin)	eBioscience	Cat#: 13-0081-85; RRID: AB_466347
Anti-mouse Streptavidin (APC)	Biolegend	Cat#: 405207
Anti-mouse Streptavidin (APC-eFlour 780)	Invitrogen	Cat#: 47-4317-82; RRID: AB_10366688
Anti-mouse Sca-1 (PE)	Invitrogen	Cat#: MA5-17890
Anti-mouse Sca-1 (PE-Cy7)	Invitrogen	Cat#: 25-5918-81
Anti-mouse c-Kit (APC)	Invitrogen	Cat#: 17-1171-82; RRID: AB_469430
Anti-mouse c-Kit (PE)	Invitrogen	Cat#: 12-1171-82; RRID: AB_465813
Anti-mouse c-Kit (PE-Cy7)	Invitrogen	Cat#: 25-1178-42; RRID: AB_10718535
Anti-mouse CD25 (APC-Cy7)	Biolegend	Cat#: 557658
Anti-mouse CD69 (PE)	eBioscience	Cat#: 12-0691-82; RRID: AB_465732
Anti-mouse CD48 (FITC)	eBioscience	Cat#: 11-0481-82; RRID: AB_465077
Anti-mouse CD150 (PE-Cy7)	eBioscience	Cat#: 25-1502-82; RRID: AB_10805742
Anti-Mouse IFNγ (PE)	eBioscience	Cat#: 12-7319-81; RRID: AB_1272169
Anti-Mouse TNFα (FITC)	eBioscience	Cat#: 11-7349-82; RRID: AB_465424
Annexin V	Biolegend	Cat#: 640908

(*Continued on next page*)

Continued

REAGENT or RESOURCE	SOURCE	IDENTIFIER
Chemicals, peptides, and recombinant proteins		
TRIzol™ Reagent	Invitrogen	Cat#: 15596026CN
Fast SYBR Green Master Mix	Clontech	Cat#: 639676
Mouse CD117 MicroBeads	Miltenyi Biotec	Cat#130-091-224
DreamTaq Green PCR Master Mix	Thermo Fisher	Cat#: K1082
DAPI	Invitrogen	Cat#D1306
Critical commercial assays		
DNeasy Blood & Tissue Kit	Qiagen	Cat#: 69506
Lineage Cell Depletion Kit	Miltenyi Biotec	Cat#: 130-110-470
TransScript® All-in-One First-Strand cDNA Synthesis SuperMix for qPCR	Trans	Cat#: AT341-01
T Cell Activation/Expansion Kit	Miltenyi Biotec	Cat#: 130-093-627
Deposited data		
RNA-seq	NOVOGENE	GEO: GSE201475
Experimental models: Organisms/strains		
Mouse: C57BL/6J	The Model Organisms Center, Inc	N/A
Mouse: B6.SJL	The Model Organisms Center, Inc	N/A
Mouse: Vav1-Cre	The Model Organisms Center, Inc	N/A
Mouse: $Phf6^{fl\text{-}R274X}$	The Model Organisms Center, Inc	N/A
Oligonucleotides		
qPCR primers see Table S1	This study	N/A
Software and algorithms		
GraphPad Prism 8	This study	N/A
FlowJo	This study	N/A
Adobe Illustrator 2021	This study	N/A
DESeq2 R package	This study	N/A

RESOURCE AVAILABILITY

Lead contact

Further information and requests for resources and reagents should be directed to and will be fulfilled by the lead contact, Xiaomin Wang (wangxiaomin@ihcams.ac.cn).

Materials availability

All unique/stable reagents generated in this study are available from the lead contact with a completed materials transfer agreement.

Data and code availability

Data

RNA-seq data have been deposited at GEO at: https://www.ncbi.nlm.nih.gov/geo/query/acc.cgi?acc=GSE201475, and are publicly available as of the date of publication. Accession numbers are listed in the key resources table.

Code

This paper does not report original code.

Other

None.

EXPERIMENTAL MODEL AND SUBJECT DETAILS

Mice

A 15.76 kb genomic DNA including Phf6 exon 8-11, two loxP sites, the FRT-flanked Neo selection cassette, and *Phf6*^{R274X} mutation in exon 8 (c.820C > T) used to construct the targeting vector by infusion (Figure S1A). Then, the mice were mated with *Vav1-Cre* transgenic mice expressing Cre recombinase under the control of the *Vav1* promoter. The *Phf6*^{R274X} mutation expressed in the hematopoietic cells at the embryonic stage with Cre activity. As expected, half of the offspring were wild-type (*Phf6*$^{fl\text{-}R274X/Y}$), and the other half were *Phf6*^{R274X} mice (*Vav1-Cre;Phf6*$^{fl\text{-}R274X/Y}$) (Figure S1B). All mice used in the experiments were male mice of 8-week-old. Mice were maintained at the specific pathogen-free (SPF) animal facility of the State Key Laboratory of Experimental Hematology (SKLEH). All animal protocols were approved by the Institutional Animal Care and Use Committee (IACUC), the Institute of Hematology, and Blood Diseases Hospital (CAMS/PUMC). All surgery was performed under sodium pentobarbital anesthesia, and every effort was made to minimize mouse suffering. The primers used for genotyping PCR are in Table S1.

METHOD DETAILS

Real time PCR

RNA was extracted using TRIzol reagent and cDNA was synthesized. RT-PCR was performed in triplicate using Fast SYBR Green Master Mix (Clontech, CA, USA), according to the manufacturer's instructions on QuantStudio 5 real-time PCR detector (ThermoFisher, USA). The primers used for RT-PCR are in Table S2.

Western blotting analysis

Western blot analysis was performed using standard protocols. Antibodies used in this study were as followings: PHF6 antibody was used at a 1:1000 dilution (Sigma). GAPDH antibody was used at a 1:1000 dilution (Cell Signaling Technology). Immunoreactive bands were visualized using enhanced chemiluminescence substrate (Bio-Rad, USA).

Bone marrow transplantation

A total of 5×10^5 BM cells was harvested from *Phf6*$^{fl\text{-}R274X/Y}$ and *Vav1-Cre;Phf6*$^{fl\text{-}R274X/Y}$ (donor mice, CD45.2$^+$) and mixed with the same number of BM cells from B6.SJL (competitor, CD45.1$^+$). The CD45.1$^+$ recipient mice were lethally irradiated (9Gy, X-ray). Every recipient mouse was transplanted with 1×10^6 mixed cells injected by lateral tail vein. The chimerism rates of CD45.2$^+$ cells in the peripheral blood of recipient mice were examined every 4 weeks. BM was examined at the fourth months after transplantation. For the serial competitive transplantation assay, 2×10^6 BM cells from primary recipients were injected into lethally irradiated CD45.1$^+$ recipient mice. All mice used were 8-10 weeks of age.

Flow cytometry

Single-cell suspensions were prepared from peripheral blood (PB), bone marrow (BM), spleen and thymus. Red blood cells from PB, BM, spleen and thymus were lysed using RBC lysis buffer. Cells were stained with antibodies at 4°C for 30min in the absence of light. Then, cells were washed and resuspended with PBS and the positive cell fragment was stained with antibodies. Data were acquired on FACS LSR II instrument (BD Biosciences, USA) and analyzed using FlowJo software 10.4. A list of antibodies used for flow cytometry is indicated in the key resources table.

T cell isolation and culture

MACS magnetic cell sorting was performed according to manufacturer's instruction (Miltenyi Biotec, Germany) to isolate Primary murine T cells from spleen. Briefly, the primary spleen cells from *Phf6*$^{fl\text{-}R274X/Y}$ and *Vav1-Cre;Phf6*$^{fl\text{-}R274X/Y}$ mice were harvested and labeled with CD3 Biotin. Anti-biotin MicroBeads were incubated for subsequent secondary labeling. After magnetic labeling, cell suspension was separated with MACS MS columns. Then, diluted cells into a density of 1×10^6 cells/ml with fresh RPMI 1640 medium (Gibco, USA) supplemented with 10% FBS, penicillin (100 U/ml), streptomycin (100 mg/ml) and mIL-2 (10ng/ml). Anti-CD3/CD28 was added to activate the primary T cells. The cells were further incubated in a 37°C incubator supplied with 5% CO_2.

Detection of CD69 and CD25 expression

For T cell activation experiments, after stimulating with anti-CD3/ CD28 for 12h or 72h, cells were harvested and washed twice with PBS. Labeled with anti-CD3, anti-CD4, anti-CD8 and anti-CD69 or anti-CD25 simultaneously at 4°C for 30 min, hen analyzed with flow cytometer.

CFSE staining

CFSE staining was performed to evaluate the proliferation of primary T cells after stimulation. 1×10^6 primary T cells/ml were pre-incubated with 5 μM CFSE at 37°C for 20 min, washed twice with 10% FBS/RPMI 1640 medium. Then stimulated with Anti-CD3/CD28 for additional 3 days. After stimulation, cells were stained with anti-CD4 and anti-CD8 at 4°C for 30min, then analyzed with flow cytometer.

Intracellular cytokine staining

After $CD3^+$ T cells stimulating with anti-CD3/CD28 for 24h, cells were stimulated with 50ng/ml PMA, 1 nM ionomycin, and GolgiPlug in 10% FBS/RPMI 1640 medium at 37 °C in 5% CO_2 incubator for 6-8 h. Cells were washed and stained with anti-CD3, anti-CD4 and anti-CD8 at 4°C for 30min. Intracellular cytokines staining were performed using Fixation/Permeabilization Solution Kit (BD Bioscience, USA) according to the manufacturer's instructions.

T cell killing assay

After $CD3^+$ T cells stimulating with anti-CD3/CD28 for 24h, 2×10^5 cells were cocultured with 2×10^4 primary spleen cells from MAL-AF9 mice for 12h. All cells were harvested, washed and stained with Annexin V at 4°C for 30min, then analyzed with flow cytometer.

RNA sequencing

BM cells were stained with lineage markers (including CD3, CD4, CD8, B220, Mac1, Gr1 and Ter119), and Lin^- cells were enriched with Biotin-antibody microbeads (Miltenyi Biotec, Cologne, Germany). Then these cells were stained with Sca-1 and c-Kit antibodies, and LSK^+ cells were sorted by the Aria III (BD Biosciences, USA). RNA was extracted using TRIzol reagent and 1μg RNA per sample was used for RNA sample preparations. Transcriptome sequencing was performed on Illumina NovaSeq 6000 platform to a total target depth of 10 million 150 bp paired end reads. Differential expression analysis was performed by DESeq2 R package (1.16.1). RNA-Seq data are available at GEO under accession number GSE201475.

QUANTIFICATION AND STATISTICAL ANALYSIS

Data were expressed as mean ± SD. $P < 0.05$ was considered statistically significant. Statistical analysis was performed using GraphPad Prism software (8.4.0). Distribution was tested using the modified Shapiro-Wilks method. When parameters followed Gaussian distribution, Student's t test was used for two groups' analyses and one-way ANOVA was used for comparing more than two groups to evaluate the statistical significance. The student's t test was performed to determine the statistical significance (* $P < 0.05$, ** $P < 0.01$, and *** $P < 0.001$). Sample size was determined according to experience or the previously published papers.